Bioresource Technology 453 (2026) 134694

Contents lists available at ScienceDirect

Bioresource Technology

journal homepage: www.elsevier.com/locate/biortech

Aerobic extracellular electron transfer in *Shewanella* spp.

Wei Chen [a,b], Biyi Zhao [a,b], Liping Dai [a,b], Junpeng Li [c], Rui Bai [b,c], Fan Yang [c], Xudong Zhou [c], Jens Ulstrup [d], Feng Zhao [b,c,*], Yong Xiao [a,b,*]

[a] *State Key Laboratory of Regional and Urban Ecology, Institute of Urban Environment, Chinese Academy of Sciences, Xiamen 361021, China*
[b] *University of Chinese Academy of Sciences, Beijing 100049, China*
[c] *State Key Laboratory of Advanced Environmental Technology, Institute of Urban Environment, Chinese Academy of Sciences, Xiamen 361021, China*
[d] *Department of Chemistry, Technical University of Denmark, DK-2800 Kgs. Lyngby, Denmark*

HIGHLIGHTS

- *S. oneidensis* MR-1 conducts EET under high dissolved oxygen (aerobic EET).
- Aerobic EET at DO $\geq$ 4 mg/L generate 5-fold higher current than under anaerobic conditions.
- Aerobic EET occurs across multiple *Shewanella* species.
- Aerobic EET reduces birnessite, informing manganese biogeochemical cycling.

GRAPHICAL ABSTRACT

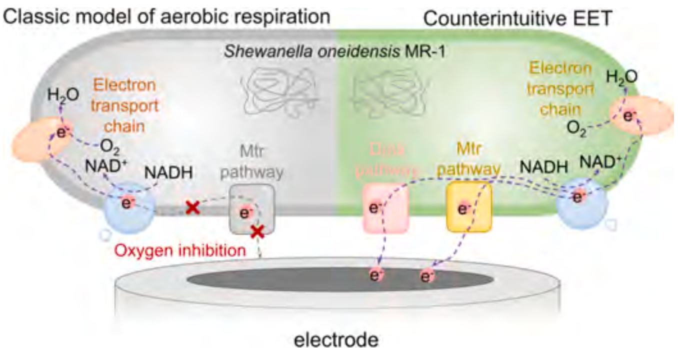

ARTICLE INFO

Keywords:
Bio-electrochemical systems
Extracellular electron transfer
High dissolved oxygen conditions
Shewanella oneidensis MR-1
Biogeochemical cycling of manganese

ABSTRACT

Microbial extracellular electron transfer (EET) can convert chemical energy directly into electron flow and is pivotal in wastewater treatment, power generation and biogeochemical cycles. However, it is widely believed that this process can only occur under anaerobic or micro-aerobic conditions, which poses severe limitations to applications of microbial EET processes. Here, we report that an EET model strain, *Shewanella oneidensis* MR-1 can activate counterintuitive EET processes to output electron flow also under high dissolved oxygen conditions, i.e. aerobic EET. Significantly, bio-electrochemical system under high dissolved oxygen conditions was found to give a 5-fold higher current density compared to commonly known anaerobic conditions. The underlying mechanism suggests that although high dissolved oxygen (>4.0 mg/L) reduces the effectiveness of electron shuttles, it supports a greater biological capacity and faster metabolic processes. We have also found that aerobic EET process can reduce effectively the manganese mineral birnessite aerobically, offering insights into the biogeochemical cycling of manganese. Furthermore, this aerobic EET processes were also identified in several *Shewanella* species.

---

* Corresponding authors at: University of Chinese Academy of Sciences, Beijing 100049, China.
E-mail addresses: fzhao@iue.ac.cn (F. Zhao), yxiao@iue.ac.cn (Y. Xiao).

https://doi.org/10.1016/j.biortech.2026.134694
Received 10 March 2026; Received in revised form 7 April 2026; Accepted 20 April 2026

1. Introduction

Extracellular electron transfer (EET) is a process in which microorganisms oxidize organic matter intracellularly and release electrons to extracellular space through an electron transport chain to obtain energy (Shi et al., 2016; Xiao et al., 2021; Xiao et al., 2017). The discovery of EET has not only broadened our understanding of the diversity of microbial respiratory pathways but also significantly expanded the variety of electron acceptors in the respiratory chain due to the unique EET mechanism (Lovley, 2006; Myers & Nealson, 1988). This holds crucial significance and application value in areas such as pollutant removal, bio-energy recovery, biosynthesis, and mineral biogeochemical cycling (Aiyer & Doyle, 2022; Bretschger et al., 2007; Harnisch et al., 2024; Lin et al., 2021; Logan, 2009).

Efficient EET processes are the key to facilitate these applications, and many studies have focused on exploring the EET mechanisms (Agee et al., 2024; Cao et al., 2021; Liu et al., 2023; Yang et al., 2020). Almost all these studies suggest that the EET processes take place under anaerobic conditions (Cao et al., 2021; Light et al., 2018; Yang et al., 2020). Microorganisms engaged in aerobic respiration typically utilize dioxygen as the electron acceptor, because dioxygen is energetically more favorable compared to other oxidizing metabolites such as Fe and Mn oxides, SO_4^{2-}, and NO_3^- in nature (Imlay, 2013; Lu & Imlay, 2021). However, anaerobic EET respiration is a low-energy yield metabolic mode and only produces limited biomass, which largely restricts technological applications of microbial EET processes.

Previous studies have promoted current generation in bioelectrochemical systems (BESs) in micro-aerobic conditions (dissolved oxygen, DO < 0.4 mg/L) (Kouzuma et al., 2012; Lu et al., 2017; Ringeisen et al., 2007; TerAvest et al., 2014). However, the rapid consumption of dioxygen by microorganisms as a function time means that EET in fact mainly occurs under anaerobic conditions. Recent studies reported that some microorganisms can reduce soluble NO_3^- and SO_4^{2-} while using dioxygen as an electron acceptor, suggesting that microorganisms can simultaneously utilize two electron acceptors (Canfield & Desmarais, 1991; Lloyd, 1993). This metabolic duality challenges the traditional dichotomy between aerobic/anaerobic respiration and motivates our central hypothesis: Certain electroactive microorganisms may execute EET under aerobic conditions. Such capability would revolutionize metal element cycling while addressing the critical oxygen sensitivity barrier hindering BESs scalability.

Herein, we present conclusive evidence that electroactive model strain *Shewanella oneidensis* MR-1 and other *Shewanella* spp. counterintuitively execute EET under high dissolved oxygen conditions (DO > 4.0 mg/L), while elucidating the underlying electron transfer mechanisms that were define as aerobic EET. The present work therefore offers to overcome the bottleneck, where dioxygen restricts widespread application of BESs, but also has highlighted new insight into the involvement of aerobic EET particularly in the biological trace element manganese under high dissolved oxygen conditions.

2. Materials and methods

2.1. Strains and culture conditions

S. oneidensis MR-1 (ATCC-700550) was kindly provided by University of Science and Technology of China. *S. lohica* (DSMZ-17748), *S. putrefaciens* (DSMZ-6067), *S. frigidimarina* (DSMZ-12253), *Bacillus subtilis* (GIM 1.258) and *Escherichia coli* K-12 (ATCC-23716) were purchased from DSMZ, Germany. *S. oneidensis* MR-1, *B. subtilis* and *E. coli* K-12 were grown aerobically in Luria-Bertani (LB, 5.0 g/L Yeast extract, 10.0 g/L Peptone, and 10.0 g/L NaCl; pH = 7.00) broth at 30℃. *S. lohica* were grown aerobically in Luria-Bertani medium (LB) broth at 20℃. *S. putrefaciens* was grown aerobically in M−948 (1 g/L “Lab-Lemco” powder, 2.0 g/L Yeast extract, 5.0 g/L Peptone, and 5.0 g/L NaCl; pH = 7.00) broth at 20℃. *S. frigidimarina* grown aerobically in 2216E medium (Bacto marine broth) broth at 25℃.

2.2. Mutant strain construction

The *S. oneidensis* MR-1 Δ*mtrA* (inhibited expression of cytochrome MtrA), Δ*cymA* (inhibited expression of cytochromes CymA), and Δ*mtrC/omcA* (inhibited expression of cytochromes MtrA and OmcA) mutants generated from strain MR-1 were kindly provided by University of Science and Technology of China (Zhu et al., 2022).

The *S. oneidensis* MR-1 Δ*sirC/cymA* (inhibited expression of cytochrome SirC and CymA) and Δ*dmsA/dmsB* (inhibited expression of cytochrome DmsA and DmsB) mutants were commissioned to be constructed by Hangzhou Fenghai Biotechnology Co., Ltd. (Zhejiang, China). The methods refer to (Gao et al., 2009). Primers used for generating PCR products for mutagenesis are listed in Supplementary Table S1.

2.3. Culture medium

Simple media used for electrochemical measurements include minimal salts medium modified from (Marsili et al., 2008). The media contained (per liter): 0.31 g NH_4Cl, 10.32 g Na_2HPO_4, 3.32 g NaH_2PO_4, 0.13 g KCl, 0.1 g $CaCl_2$, 0.1 g $MgSO_4·7H_2O$, plus 10 mL of a mineral mix (containing per liter: 1.5 g NTA, 0.1 g $MnCl_2·4H_2O$, 0.3 g $FeSO_4·7H_2O$, 0.17 g $CoCl_2·6H_2O$, 0.1 g $ZnCl_2$, 0.04 g $CuSO_4·5H_2O$, 0.005 g $AlK(SO_4)_2·12H_2O$, 0.005 g H_3BO_3, 0.09 g Na_2MoO_4, 0.12 g $NiCl_2$, and 0.02 g $NaWO_4·2H_2O$). The final pH was about 7.00. After autoclaving, filter-sterilized casamino acids were added (0.002%), and plus 1 mL of vitamins (containing per liter: 0.05 g 4 Aminobenzoic acid, 0.01 g D (+) biotin, 0.1 g Nicotinic acid, 0.025 Ca-D (+) pantothenate, 0.25 g Pyridoxamine dihydrochloride, 0.05 g Thiaminium dichloride, 0.05 g Cyanocobalamin).

2.4. Operation of three-electrode BESs

A double chamber three-electrode BESs was used to monitor electric current generated by *S. oneidensis* MR-1 and other strains under constant potential (+200 mV). The BESs were equipped with a carbon felt (or carbon paper) working electrode (4 cm^2), an Ag/AgCl reference electrode, and a carbon felt counter electrode (9 cm^2). The BESs reactor has an air inlet and an air outlet. The air inlet was connected with a sterile 0.22 µm filter, and the air outlet covered with a breathable sealing film. For aerobic BESs measurements, an air pump and a flow meter were used to control the air flow into the reactor at 40 mL/min. The medium in the electrochemical chamber was mixed using a magnetic stir bar (100 rpm) throughout the experiment. 20 mM 60% (v/v) sodium DL-lactate ($C_3H_6O_3$) solution (cultivation of *B. subtilis* and *E. coli* K-12 added 20 mM glucose) acted as the electron donor, and 120 mL simple medium as electrolyte. The overnight culture of *S. oneidensis* MR-1 and other cultures were washed three times by centrifugation (5000·*g*, 5 min) using 50 mM PBS, and then inoculated 1% into the BESs. The electrochemical cells were connected to an eight-channel potentiostat (CHI1000, CHI Instruments, Shanghai, China) controlled by a computer.

2.5. Biomass measurements

The biomass was determined by the protein concentration using a BCA assay kit.

2.6. SEM sample preparation

Samples were collected and placed in 2.5% glutaraldehyde (Diluted with 50 mM PBS, pH = 7.00), kept at 4°C for 2 h, the pellets then washed twice with 0.5% NaCl, followed by dehydration with 30%, 50%, 70%, 90%, and 100% ethanol, and finally dried with a critical point drier and observed by SEM (S-4800, Hitachi, Japan).

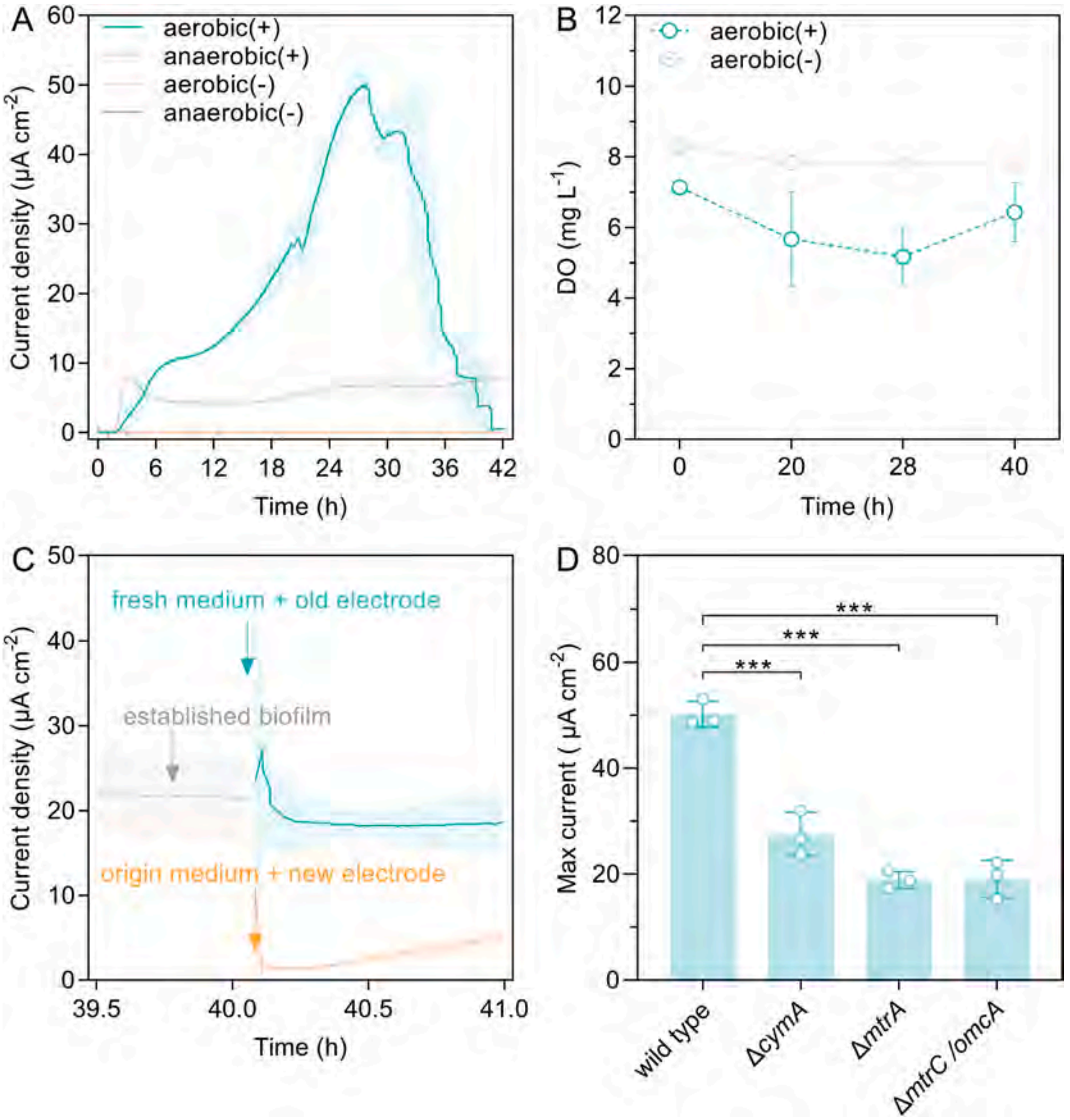

Fig. 1. Unexpected aerobic current generated from *S. oneidensis* MR-1 inoculated BESs. (A) Chronoamperometry from *S. oneidensis* MR-1 inoculated BESs using carbon felt (2*2 cm^2) and carbon felt (2*3 cm^2) as working and counter electrode, respectively. An Ag/AgCl electrode is the reference electrode. Aerobic reactors with 40 mL/min of air input. Electron donor (lactate) was present in (+) or absent from (−) the medium. (B) The dissolved dioxygen (DO) in the aerobic BESs. Electron donor (lactate) was present in (+) or absent from (−) the medium. (C) Current generation in the medium replacement experiment using established *S. oneidensis* MR-1 biofilms in aerobic BESs. Grey trace represents the oxidation current from the established *S. oneidensis* MR-1 biofilms, blue trace the oxidation current from the established *S. oneidensis* MR-1 biofilms after being transferred to fresh medium. Orange trace represents the oxidation current from abiotic electrodes in the original medium. (D) Maximum current from aerobic chronoamperometry with wild-type and mutant *S. oneidensis* MR-1. All data represent mean values, with error bars representing one standard deviation (n = 3 biologically independent samples). Statistical analysis was conducted with one-way ANOVA test: ***, $p < 0.001$.

2.7. Dissolved dioxygen detection

Dissolved dioxygen was tested by a water quality meter (Instrument AZ86031, China).

2.8. ATP quantification

ATP levels were measured using a firefly luciferase based ATP assay kit (Beyotime, S0027). *S. oneidensis* MR-1 was incubated in aerobic/anaerobic BESs at 30°C for 28 h. The biofilm on the electrode was resuspended using 50 mM PBS and then centrifuged (5000·g, 5 min) to collect bacterial cells. The suspended bacterial cells were collected by centrifugation, and the supernatant removed. ATP assay lysis buffer (200 μL) was added to the centrifuge tube containing the bacterial cell precipitate at 4°C and mixed thoroughly. The solution was centrifuged at 12,000 g for 5 min (4°C). The ATP assay working dilution (100 μL) was mixed with the supernatant (20 μL) after lysis. The brightness was measured immediately using a monochromator enzyme marker, and a standard curve using an ATP standard solution prepared by the same method. The protein concentration of the solution was measured using the BCA assay kit.

2.9. NAD^+/NADH quantification

S. oneidensis MR-1 was incubated in aerobic/anaerobic BESs at 30°C for 28 h. Bacterial cells were collected from the supernatant and working electrode using the method described, and their intracellular NAD^+/NADH ratios determined using a NAD^+/NADH –Glo Kit (Promega, Madison, WI, USA) according to the manufacturer’s instructions.

2.10. Label-free quantitative proteomic analysis

To analyze the changes in proteomics of aerobic EET biofilms, suspended microorganisms in the aerobic electrochemical system, biofilms in the aerobic open circuit system, and anaerobic biofilms were set up as controls. The largest current difference of electrode microorganisms in 28 h was selected as proteomics samples. Three biological replicates were investigated separately. The proteomics samples were collected and subjected to Label-free Quantitative Proteomic Analysis by Shanghai Applied Protein Technology Co. Ltd. (Shanghai, China).

The extraction and digestion of proteins were based on a published method (Gang et al., 2019). Each sample was injected for nanoLC-MS/MS analysis. LC-MS/MS analysis was carried out using a Q Exactive mass spectrometer (Thermo Scientific) coupled to Easy nLC (Proxeon Biosystems, now Thermo Fisher Scientific) for 120 min. Statistical analysis of MaxQuant label-free quantitation data was performed with the artMS Bioconductor package3 which performs the relative quantification of protein abundance using the MSstats Bioconductor package. The abundance of proteins missing from one condition but found in more than 2 biological replicates of the other condition for any given comparison were estimated by imputing intensity values from the lowest observed MS1-intensity across 5 samples and *p*-values were randomly assigned to those between 0.05 and 0.01 for illustration purposes.

2.11. Bacterial community analysis

The inoculum, biofilm, and the supernatant in the electrochemical system were collected by centrifugation for DNA extraction. The 16S rRNA gene sequencing was carried out using an Illumina platform by Biomarker Technologies Corporation (Beijing, China), following the method described in our previous report (Xiao et al., 2021).

2.12. Analysis of flavins

Electrolyte of 2 mL in three-electrode systems was collected, and the concentration was determined by high performance liquid chromatography following our previous report (Xiao et al., 2021).

2.13. Aerobic bio-reduction of birnessite

Synthetic birnessite was prepared as described (McKenzie, 1971). A 50 mL concentrated HCl was added dropwise with stirring to a boiling solution containing 0.2 mol $KMnO_4$ in 350 mL ultrapure water. After all the HCl was added, the solution was left to boil for an additional 30 min. The cooled suspension was centrifuged (3500g, 10 min) and purified with ultrapure water to pH 7.00. Additional washing removed residual K, Cl, and aqueous Mn ions, by dialysing the oxide against ultrapure water using a 14 kDa molecular mass cut-off dialysis membrane. After completion of dialysis, birnessite was dried at 60℃ and stored in the dark.

A 100 mL blue-capped bottle was used as the reactor. In aerobic washing, an air pump and a flow meter were used to control the air flow into the reactor at 40 mL/min. The medium in the blue-capped bottle was stirred with a magnetic stir bar (100 rpm) throughout the experiment. 20 mM 60% (v/v) sodium DL-lactate ($C_3H_6O_3$) solution added acted as the electron donor and 1 mM birnessite added as the electron acceptor. The overnight culture of *S. oneidensis* MR-1 and mutants using Luria-Bertani medium were washed three times by centrifugation (5000·g, 5 min) using 50 mM PBS and then inoculated 1% into the reactor. Abiotic control without inoculation was used. The reactor was run at a constant temperature of 30°C.

2.14. Quantification of Mn (III/IV) oxides and dissolved Mn

Mn (III/IV) oxides were quantified by monitoring the absorbance (620 nm) of the samples after addition of 5 times the volume of the colorimetric reagent Leucoberlin blue I (LBB, Sigma-Aldrich) (Trouwborst et al., 2006). To test dissolved Mn in the incubation solution, 1.5 mL samples were collected, centrifuged (12,000g, 5 min) and filtered (0.22 μm) to remove birnessite and cells. The samples were then quantified by inductively coupled plasma optical emission spectrometry (ICP-OES) (Optima 7000DV, PerkinElmer, USA).

2.15. Statistical analyses

The statistical analyses and graphs were performed using GraphPad Prism 9.5.1(733). For comparisons between two groups, significance was determined using a two-tailed unpaired Student's *t*-test, while for comparisons among three or more groups, one-way ANOVA test was employed (ns, $p \geq 0.05$; *, $p \leq 0.05$; **, $p \leq 0.01$; ***, $p \leq 0.001$).

3. Results and discussion

3.1. Bioelectricity generation from aerobic BESs

We have monitored the electrochemical current generation from *S. oneidensis* MR-1 using three-electrode BESs, and evaluated the microbial EET capacity. By applying a potential of + 0.2 V (versus KCl saturated Ag/AgCl, unless otherwise stated) on the working electrode (4 cm^2 carbon felt), the anaerobic BESs (Fig. S1a) produced a maximum current of 8 μA cm^{-2} which accords with previous studies (Xiao et al., 2021; Yang et al., 2020). However, unexpectedly a maximum current higher than 50 μA cm^{-2} (Fig. 1A, and Supplementary Movie) was generated from aerobic BESs (input 40 mL/min air) (Fig. S1b). In addition, the open-circuit potential decreased as *S. oneidensis* MR-1 grew, with the electrode potential declining from +0.150 V to −0.540 V (Fig. S2). To further evaluate the sustained operational performance of the system, we conducted microbial fuel cell experiments over three operation cycles (Fig. S3), and the results showed that the system maintained stable voltage output throughout repeated cycles, with rapid recovery after sodium lactate addition when the voltage dropped to a low level.

Chronoamperometry without *S. oneidensis* MR-1 inoculation showed no current yield from oxidation of lactate or its possible metabolic acetate and formate intermediates (Fig. S4). This means that *S. oneidensis* MR-1 must be what produces electricity in the aerobic BESs. We then recorded dissolved dioxygen (DO) concentration at around 5.0 mg/L in the aerobic BESs at 28 h, when the BESs delivered the maximum current (Fig. 1B). Previous studies have shown that only micro-aerobic conditions (DO < 0.4 mg/L) can promote BES current generation, but the rapid consumption of dioxygen by microorganisms means that EET actually occurs under anaerobic conditions (Kouzuma et al., 2012; Lu et al., 2017; Ringeisen et al., 2007; TerAvest et al., 2014). We used a carbon paper with a thickness of only 0.1 mm as working electrode to make sure that there are no anaerobic regions caused by depletion of oxygen by outer layer bacterial cells, because *S. oneidensis* MR-1 exists as a single layer of dispersed cells on the carbon paper (Fig. S5). Consistent with carbon felt electrodes, the results showed that aerobic EET is still 3-fold higher current density than anaerobic EET.

S. oneidensis MR-1 has been widely reported to possess two EET pathways, a direct pathway via outer-membrane *c*-type cytochromes and an indirect pathway via electron shuttles such as riboflavin (Norman et al., 2023). Flavin measurement showed that aerobic BESs produced 0.29 μM of flavin mononucleotide and 0.03 μM of riboflavin, while anaerobic BESs produced only 0.05 μM of flavin mononucleotide (Fig. S6). These results suggest that indirect electron transfer may contribute to the aerobic EET. However, the medium replacement experiment (Marsili et al., 2008; Mevers et al., 2019) showed that about 97% of the current was immediately recovered after replacement with fresh medium without flavins, suggesting that soluble electron shuttles make only a limited contribution to the aerobic EET current and that the current was mainly derived from the electrode biofilm (Fig. 1C). Only

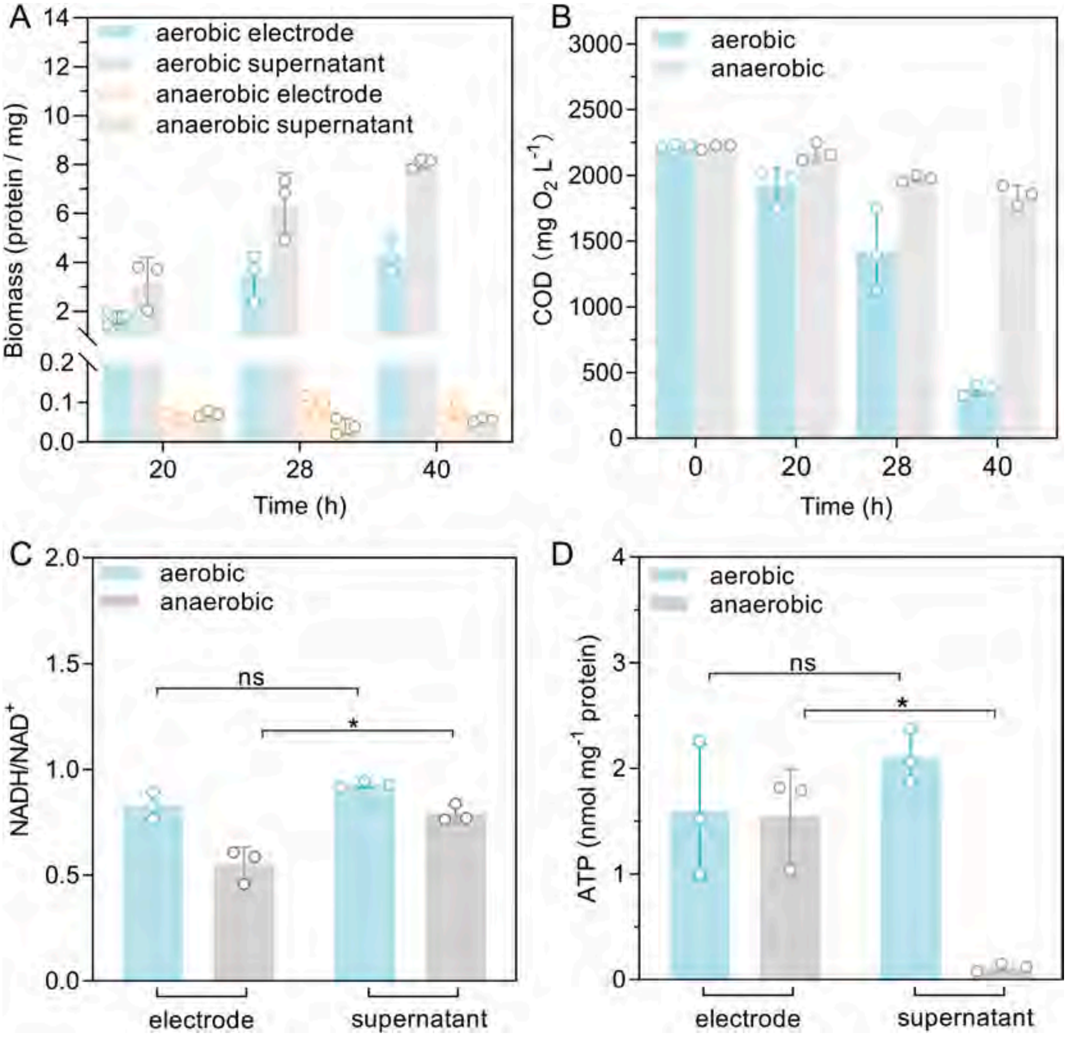

Fig. 2. The metabolic basis of *S. oneidensis* MR-1 in BESs. (A) Production of protein-based biomass from aerobic and anaerobic BESs at 20, 28, and 40 h, respectively. (B) Chemical dioxygen demand at different times in aerobic and anaerobic BESs. (C) NADH / NAD$^+$ ratios and (D) ATP production per mg of protein at the maximum current density. All data represent mean values, with error bars representing one standard deviation (n = 3 biologically independent samples). Statistical analysis was conducted with paired two-tailed t tests: ns, $p > 0.05$; *, $p < 0.05$.

7% of the current was immediately recovered when the original medium was added into aerobic BESs with a new electrode, further indicating that the electrode biofilm was primarily responsible for aerobic EET.

Cyclic voltammetry results showed that aerobic and anaerobic biofilms exhibited differences in redox peak, suggesting that the electron transfer pathway may differ under aerobic conditions (Fig. S7). Considering that under anaerobic conditions, *S. oneidensis* MR-1 uses *c*-type cytochromes of CymA, MtrA, MtrC and OmcA to transport electrons to extracellular electron acceptors in the direct EET pathway (Bretschger et al., 2007), we introduced three mutants Δ*cymA*, Δ*mtrA*, and Δ*mtrC/omcA* to investigate the roles of these cytochromes in aerobic EET. Compared with the wild-type strain, the maximum current in aerobic BESs inoculated with Δ*cymA*, Δ*mtrA*, and Δ*mtrC/omcA* mutants decreased by about 45%, 60%, and 60%, respectively (Fig. 1D). This suggests that CymA, MtrA, MtrC and OmcA are important in the aerobic EET process. However, under anaerobic condition mutants of Δ*mtrA* and Δ*mtrC/omcA* generated less than 12% of the current from wild-type *S. oneidensis* MR-1 (Fig. S8). These results strongly suggest that besides CymA, MtrA, MtrC and OmcA, other proteins also important in aerobic EET.

3.2. Metabolic basis of aerobic EET

Biomass produced is one of the most important factors representing BES performance. The growth curves (optical density at 600 nm, OD_{600}) showed that the population density of *S. oneidensis* MR-1 under aerobic conditions is 3.6-fold higher than under under anaerobic conditions (Fig. S9). We first examined the biomass in different BESs using a protein-based method (BCA Protein Assay) and found 36 and 162-fold biomass increase at the working electrodes and supernatant, respectively in the aerobic BESs, at 28 h compared with the anaerobic BESs (Fig. 2A). This result was supported by scanning electron microscopy (Fig. S10). The rapid accumulation of biomass in aerobic BESs accords with efficient attenuation of chemical dioxygen demand (COD), an index representative of the amount of organics converted. COD measurements showed that aerobic BESs removed up to 83% of COD in 40 h, while anaerobic BESs removed only 13% (Fig. 2B). These results indicate that the aerobic EET process can recover higher density of energy compared with anaerobic EET processes, due to faster substrate consumption and higher biomass accumulation.

We attempted next to understand the aerobic *S. oneidensis* MR-1 EET respiration by comparing the NADH/NAD$^+$ ratios and ATP levels at the highest current density. Aerobic respiration normally has a low NADH/NAD$^+$ ratio, favoring the oxidized state and high energy production,

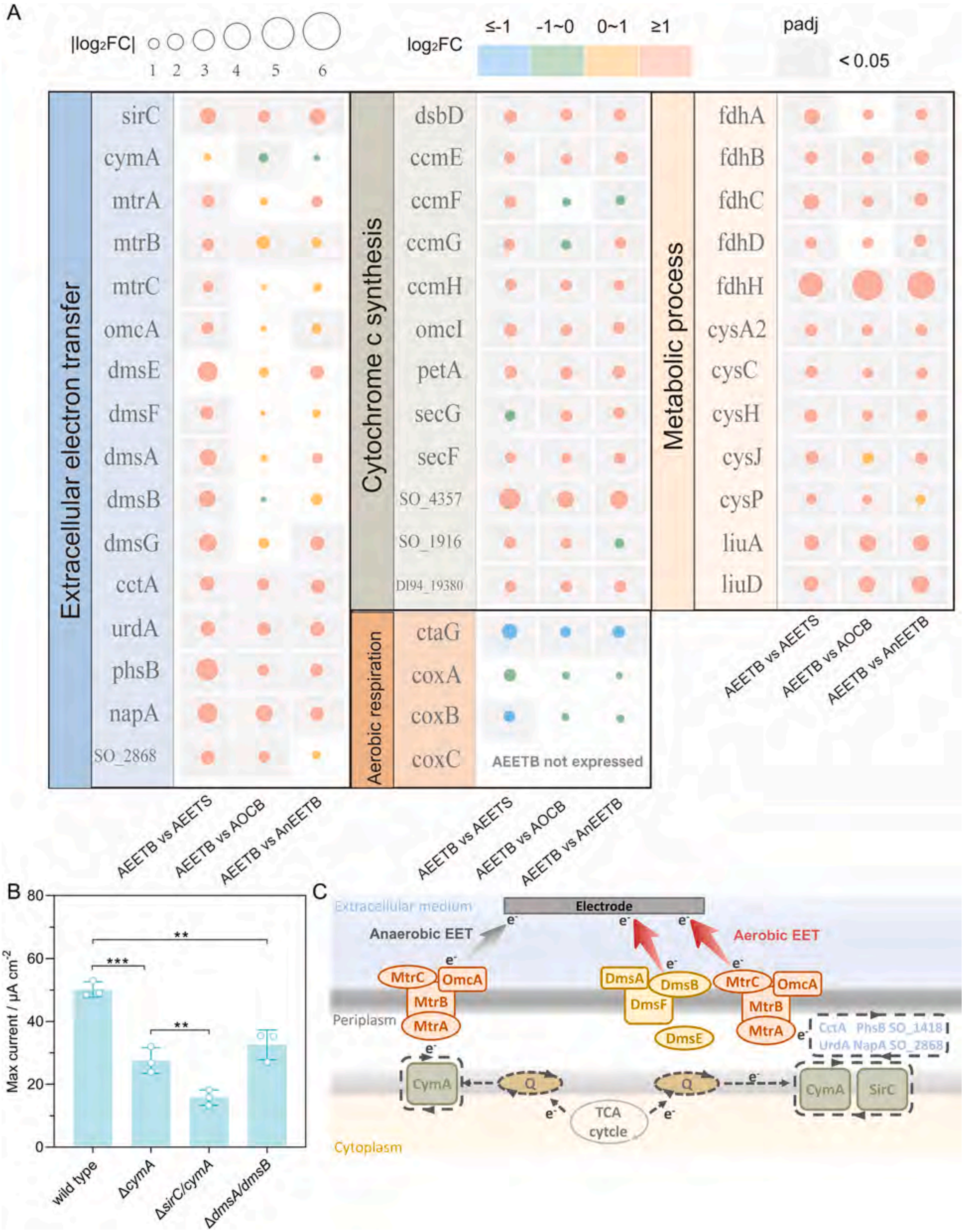

Fig. 3. Investigation of the aerobic EET mechanism. (A) Proteomics analysis of proteins associated with aerobic EET metabolism, mainly including the EET process, cytochrome *c* synthesis, metabolic processes and aerobic respiration. AEETB represents electrode biofilm in aerobic BESs, AEETS supernatant in aerobic BESs, AOCB aerobic biofilm on the electrode without applied potential (i.e. open circuit), and AnEETB electrode biofilm in anaerobic BESs. The size of the circles represents the upregulation fold of the relevant proteins; red represents upregulation, green downregulation. The detailed fold change values of the proteins are listed in the Supplementary Materials. (B) Maximum current recorded by aerobic BESs inoculated with wild-type and mutant *S. oneidensis* MR-1. (C) Proposed *S. oneidensis* MR-1 metabolic aerobic EET pathways. Statistical analysis conducted with paired two-tailed t tests: ** $p < 0.01$; *** $p < 0.001$.

whereas anaerobic respiration has a high NADH/NAD$^+$ ratio favoring the reduced state and low energy production (Holm et al., 2010; Tejedor-Sanz et al., 2022). Our results suggest that the NADH/NAD$^+$ ratios in the biofilm of anaerobic BESs is significantly lower than that in the supernatant of anaerobic BESs (Fig. 2C), indicating that EET can promote *S. oneidensis* MR-1 anaerobic metabolism processes. We found similar NADH/NAD$^+$ ratios between biofilm and supernatant in aerobic BESs, which may indicate that the metabolic state of aerobic EET is similar to aerobic respiration. The ATP results were consistent with the NADH/NAD$^+$ ratios results. The biofilm ATP levels in anaerobic BESs, are significantly higher than in the anaerobic supernatant, whereas similar ATP levels between the aerobic BESs biofilm and supernatant (Fig. 2D) were found. The NADH/NAD$^+$ ratios and ATP levels thus suggest that the metabolic efficiency of aerobic EET is similar to aerobic respiration.

3.3. *The mechanism of aerobic EET*

Proteomics analysis showed that protein expression was significantly different within *S. oneidensis* MR-1 aerobic BES biofilms (denoted as AEETB) compared with suspended microorganisms in aerobic BESs (denoted as AEETS), the biofilm in the aerobic open-circuit reactor (denoted as AOCB), as well as the electrode biofilms of anaerobic BESs (denoted as AnEETB). The analysis further showed that the expression of 279, 248 and 222 proteins is upregulated ($\log_2$ Fold change > 1) (Fig. S11). This is notable, as many of the upregulated proteins relate directly to EET, *c*-type cytochrome synthesis, and energy metabolism (Fig. 3A). We consider these proteomics outcomes in turn below.

The *c*-type cytochromes are the primary outer membrane transmitters for transporting intracellular electrons directly to external electron acceptors, and their expression levels are critical for EET efficiency (Shi et al., 2016). Specifically, Mtr pathway *c*-type cytochromes (MtrA, MtrB, MtrC, and OmcA) in AEETB samples related to EET were found to be significantly upregulated compared with AEETS. By directly comparing the cell colors of AEETB and AEETS samples, the more strongly red (Feng et al., 2019) color of the AEETB sample confirms the upregulation of *c*-type cytochromes expression in AEETB compared to AEETS (Fig. S12). This result is consistent with the validation results of the mutant (Fig. 1D), indicating that the proteins in the Mtr pathway are crucial in aerobic EET. Simultaneously, the Dms pathway (DmsA, DmsB, DmsE, DmsF, and DmsG) *c*-type cytochromes, which were originally identified in studies of dimethyl sulfoxide reduction (Gralnick et al., 2006) and have also been implicated in the extracellular reduction of multiple electron acceptors (Chen et al., 2026; Hou et al., 2024), were also found to be significantly upregulated (Fig. 3A). Considering that the proteins in the Dms pathway were significantly upregulated during aerobic EET, with protein structural similarities with the Mtr pathway, and that the Mtr pathway-deficient strain still retained 38% of the current during aerobic EET (Fig. 1D), we found it highly likely that the Dms pathway is important in aerobic EET (Fig. 3C).

More importantly, the expression of SirC, which has a function similar to that of CymA (Cordova et al., 2011), was found 4-fold upregulated in AEETB, compared to AnEETB. Considering that mutant Δ*cymA* retained 45% of the maximum current in aerobic BESs, SirC might be as important as CymA in the aerobic EET process. In addition, FccA and CctA are important periplasmic electron transfer proteins in the EET pathway of *S. oneidensis* MR-1 (Shi et al., 2016). We also detected a significant expression upregulation of CctA along with certain FccA homologous in AEETB samples, compared with AEETS, AOCB and AnEETB. The expression of *c*-type cytochromes requires a cytochrome *c* maturation (Ccm) system which covalently links the heme *b* moiety to apo-cytchrome *c* to form a complete cytochrome *c* (Su et al., 2020). We observed an upregulated expression of the Ccm system as well as of the DsbD and *Sec* systems in AEETB, compared with AEETS, AOCB and AnEETB (Fig. S13). Moreover, the expression of key proteins in the formate (FdhA, FdhB, FdhC, FdhD and FdhE) and sulfate (CysA2, CysC, CysH, CysJ and CysP) metabolic pathways were found to be significantly upregulated (Fig. 3A), indicating that the metabolic activity of *S. oneidensis* MR-1 in AEETB is higher in AEETB than in AEETS, AOCB and AnEETB. To summarize, the expression upregulation of outer membrane-associated *c*-type cytochromes and proteins related to intracellular metabolic activity has provided a solid basis for aerobic EET.

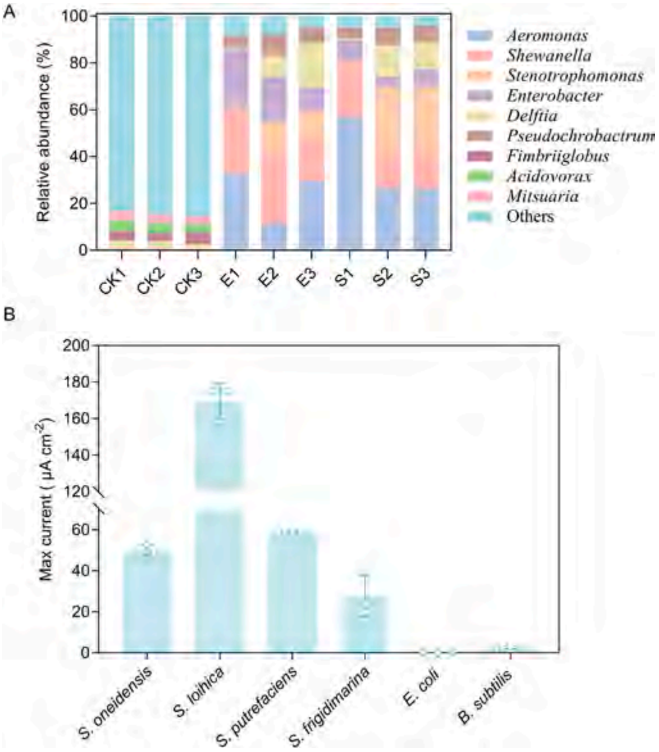

Fig. 4. Prevalence of aerobic EET in *Shewanella* spp. (A) Diversity analysis of mixed bacterial communities in aerobic BESs. CK1-3 represents the inoculant, E1-3 the electrode biofilm in aerobic BESs at 48 h, S1-3 the supernatant in aerobic BESs at 48 h. (B) Maximum chronoamperometry current in aerobic BESs inoculated with representative strains of *S. loihica*, *S. putrefaciens*, *S. frigidimarina, Escherichia coli* and *Bacillus subtilis*. The data represent mean values with error bars representing one standard deviation (n $\geq$ 3).

The proteomics analysis provides valuable clues to how *S. oneidensis* MR-1 undergoes aerobic EET. We developed two mutants of Δ*sirC/cymA* and Δ*dmsA/dmsB* to further illustrate this process. Aerobic chronoamperometry showed that compared with the wild-type strain, the maximum aerobic current density of mutants of Δ*cymA* and Δ*sirC/cymA* mutants decreased by about 45% and 69%, respectively (Fig. 3B). In addition, the maximum aerobic current density of mutant Δ*dmsA/dmsB* decreased by 35%, compared to the wild-type in aerobic BESs. Anaerobic chronoamperometry showed that the maximum current density of Δ*sirC/cymA* was not significantly different from that of Δ*cymA*, and the maximum current density of Δ*dmsA/dmsB* was not significantly different from that of the wild-type (Fig. S14). This further point to the importance of the protein SirC and the Dms pathway in aerobic EET. These results therefore substantiate that aerobic EET of *S. oneidensis* MR-1 is dominated by an EET network consisting of the inner membrane *c*-type cytochrome CymA and SirC proteins and of the outer membrane *c*-type cytochromes Mtr (MtrA, MtrB, MtrC, OmcA) and Dms pathways (DmsA, DmsB, DmsE, DmsF).

3.4. *Prevalence of aerobic EET*

Aerobic respiration can produce much more energy than anaerobic respiration (including anaerobic EET respiration). Aerobic respiration

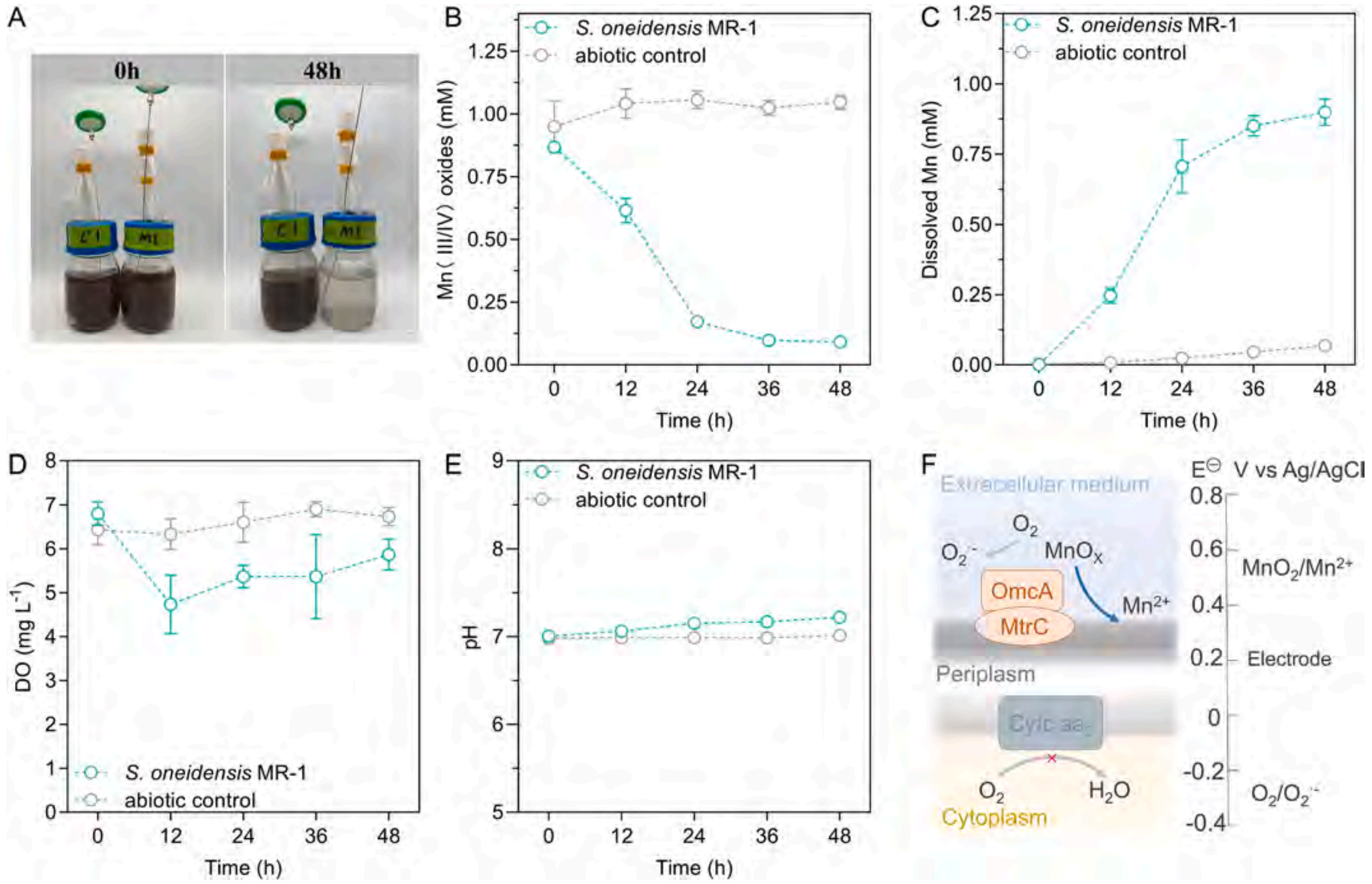

Fig. 5. Aerobic reduction of the manganese mineral birnessite by *S. oneidensis* MR-1. (A) Birnessite transformed by *S. oneidensis* MR-1 in reactors with air pumped in at 40 mL/min. C1 represents an abiotic control; M1 was inoculated with *S. oneidensis* MR-1. (B) Variation of Mn (III/IV) oxide concentration over different time periods. (C) Quantification of dissolved Mn in abiotic control and reactors inoculated with *S. oneidensis* MR-1. (D) The dissolved dioxygen (DO) in all reactors was higher than 4 mg/L. (E) pH from each sample with and without inoculation of supernatant *S. oneidensis* MR-1. (F) Standard reduction potentials for possible reactions of *S. oneidensis* MR-1 in aerobic EET. The data represent mean values, error bars one standard deviation (n = 3). *S. oneidensis* MR-1 and abiotic control represent reactors inoculated with and without *S. oneidensis* MR-1.

may yield reactive oxygen species and consequently impose colossal oxidative stress on microorganisms. Oxidative damage can have a devastating effect on the structure and activity of proteins, and may even lead to cell death (Ezraty et al., 2017). Recent studies have shown that the Mtr pathway of *S. oneidensis* MR-1 is useful in direct reduction of dioxygen (Chen et al., 2023). The upregulation of proteins associated with Mtr pathways may therefore be a mechanism by which *S. oneidensis* MR-1 effectively utilizes aerobic EET to reduce dioxygen outside the cell, thus attenuating the dioxygen entry into the cell. More importantly, the expression of CoxB, a protein closely associated with aerobic respiration, is significantly downregulated in biofilm cells (AEETB) compared with suspended cells (AEETS). Another similar CoxC protein is not expressed in AEETB only (Fig. 3A), meaning that *S. oneidensis* MR-1 aerobic respiration in electrode biofilms may be reduced. Surprisingly, CoxC protein was also found to be expressed in the absence of dioxygen in AnEETB, suggesting that the absence of CoxC protein expressed in AEETB *S. oneidensis* MR-1 may be an active response to attenuate reactive oxygen species.

Whether aerobic EET occurs universally is an intriguing question. We addressed this question by inoculating three aerobic BESs with mixed bacteria from a wastewater treatment plant (Anshun City, Guizhou). We were able to produce a maximum current of about 22 μA cm^{-2} (Fig. S15). *Shewanella* spp. were enriched in both supernatants and electrode biofilms of aerobic BESs (Fig. 4A), demonstrating that aerobic EET does contribute to the survival of *Shewanella* spp. at high DO. Most *Shewanella* spp. are able to reduce metallic minerals, and *S. loihica*, *S. putrefaciens* and *S. frigidimarina* have similar Mtr pathways as *S. oneidensis* MR-1 (Fredrickson et al., 2008). We propose that these bacteria are also able to conduct aerobic EET. Significant aerobic current generation from BESs inoculated with *S. loihica*, *S. putrefaciens*, and *S. frigidimarina*, further confirmed the prevalence of aerobic EET in *Shewanella* spp. (Fig. 4B). We also inoculated *Escherichia coli* and *Bacillus subtilis* into aerobic BESs. Although these bacteria have a large biomass in these aerobic BESs, they do not possess Dms and Mtr pathways and generate only negligible current (Fig. 4B). These results confirm that Dms and Mtr pathways are more crucial for aerobic EET than high biomass, highlighting the widespread presence of aerobic EET in many *Shewanella* spp. with Dms and Mtr pathways.

3.5. S. oneidensis MR-1 and aerobic reduction of manganese oxide minerals (birnessite)

Manganese (Mn) is a core biological trace element acting as a cofactor, in photosystem II of higher plants and for a number of enzymes with antioxidant and metabolic functions and is essential for all forms of life. Mn(II) and Mn(IV) oxides are typically present in soluble and insoluble forms, respectively. Microbial EET is believed to participate in the biogeochemical cycle of Mn, for example by reducing anaerobically manganese oxide MnO_2 to Mn^{2+} (Myers & Nealson, 1988). Under aerobic conditions, manganese is often present in the form of biologically inaccessible and insoluble manganese oxides, with birnessite being one of its natural forms. In our present study, synthetic solid birnessite (Mn

(III/IV), Fig. S16) was found to decrease from about 1.0 to 0.2 mM in aerobically grown *S. oneidensis* MR-1 culture. The solution became clear after 48 h cultivation (Fig. 5A and B). Ionic Mn(II) increased in parallel from 0 to about 0.9 mM in the culture with DO concentration ranging from 4.0 to 6.0 mg/L (Fig. 5C and D). Since pH was maintained at 7.0–7.2 (Fig. 5E), these results mean that ionic Mn(II) is formed by reduction of Mn(IV) in the aerobically grown *S. oneidensis* MR-1 system. Furthermore, the manganese oxide reduction rate was significantly reduced in mutant Δ*mtrC/omcA* (Fig. S17), suggesting that manganese oxides reduction is largely dependent on the EET pathway.

The bioreduction of minerals is generally believed to proceed under anaerobic conditions because of the high dioxygen redox potential (Fig. 5F), making it hard for metal oxides to compete thermodynamically with dioxygen for electrons. However, *S. oneidensis* MR-1 could interrupt the expression of CoxC protein (associated with intracellular reduction of O_2 to H_2O) in EET respiration (Fig. 4A), where extracellular *c*-type cytochromes (MtrC and OmcA) are exploited to reduce O_2 to $O_2^{\cdot-}$ (−0.357 V). Electrons readily flow from low potential to high potential such as birnessite (+0.532 V) and electrochemical electrodes (+0.20 V) (Fig. 5F). We therefore conclude that birnessite or an electrode can indeed receive electrons, i.e. be aerobically reduced by *S. oneidensis* MR-1 and other *Shewanella* spp.

4. Conclusion

Our study has disclosed an efficient, and novel microbial EET process focused on the strain *S. oneidensis* MR-1. The process rests on aerobic EET which produced 5-fold higher current than that from anaerobic EET. While high dissolved oxygen (DO > 4.0 mg/L) reduces the effectiveness of electron shuttles, it supports greater biological capacity and faster metabolic processes. We have explored the aerobic EET network mechanisms in detail and shown that Mtr and Dms pathways are primary contributors to the aerobic bioelectricity generation. Our discovery and detailed mechanistic mapping of aerobic EET further suggest that microorganisms participate broadly in the biogeochemical cycles of metallic elements under aerobic conditions using EET processes in much the same way they do anaerobically. Broader development of aerobic EET will offer new opportunities for integrating microbial electrochemical processes into already aerated systems and other oxygen-rich environments, where anaerobic EET is less readily applicable. Aerobic EET can thus be expected to promote microbial electrochemical techniques in energy recovery, pollution remediation, and other high-technology applications.

CRediT authorship contribution statement

Wei Chen: Writing – original draft, Visualization, Methodology, Formal analysis, Data curation. **Biyi Zhao:** Methodology, Data curation. **Liping Dai:** Validation, Data curation. **Junpeng Li:** Investigation, Data curation. **Rui Bai:** Investigation, Data curation. **Fan Yang:** Resources. **Xudong Zhou:** Investigation, Data curation. **Jens Ulstrup:** Writing – review & editing. **Feng Zhao:** Writing – review & editing, Supervision, Project administration, Methodology, Funding acquisition, Conceptualization. **Yong Xiao:** Writing – review & editing, Supervision, Project administration, Methodology, Funding acquisition, Conceptualization.

Declaration of competing interest

The authors declare that they have no known competing financial interests or personal relationships that could have appeared to influence the work reported in this paper.

Acknowledgements

The authors thank Prof. Han-Qing Yu, and Dr. Dong-Feng Liu for kindly providing the mutants Δ*cymA*, Δ*mtrA*, and Δ*mtrC/omcA*. This work was supported by the National Natural Science Foundation of China (22276183, 22025603, 42021005), the Natural Science Foundation of Fujian for Distinguished Young Scholars (2021J06036), Institute of Urban Environment, Chinese Academy of Sciences (IUE-JBGS-202212), the CAS Key Laboratory of Urban Pollutant Conversion Joint Research Fund (KLUPC-2020-4), and the Youth Innovation Promotion Association, Chinese Academy of Sciences (Y2022082).

Appendix A. Supplementary data

Supplementary data to this article can be found online at https://doi.org/10.1016/j.biortech.2026.134694.

Data availability

Data will be made available on request.

References

Agee, A., Pace, G., Yang, V., Segalman, R., Furst, A.L., 2024. Mixed conducting polymers alter electron transfer thermodynamics to boost current generation from electroactive microbes. J. Am. Chem. Soc. 146 (29), 19728–19736.

Aiyer, K., Doyle, L.E., 2022. Capturing the signal of weak electricigens: a worthy endeavour. Trends Biotechnol. 40 (5), 564–575.

Bretschger, O., Obraztsova, A., Sturm, C.A., Chang, I.S., Gorby, Y.A., Reed, S.B., Culley, D.E., Reardon, C.L., Barua, S., Romine, M.F., Zhou, J., Beliaev, A.S., Bouhenni, R., Saffarini, D., Mansfeld, F., Kim, B.-H., Fredrickson, J.K., Nealson, K.H., 2007. Current production and metal oxide reduction by *Shewanella oneidensis* MR-1 wild type and mutants. Appl. Environ. Microbiol. 73 (21), 7003–7012.

Canfield, D.E., Desmarais, D.J., 1991. Aerobic sulfate reduction in microbial mats. Science 251 (5000), 1471–1473.

Cao, B., Zhao, Z., Peng, L., Shiu, H.-Y., Ding, M., Song, F., Guan, X., Lee, C.K., Huang, J., Zhu, D., Fu, X., Wong, G.C.L., Liu, C., Nealson, K., Weiss, P.S., Duan, X., Huang, Y., 2021. Silver nanoparticles boost charge-extraction efficiency in *Shewanella* microbial fuel cells. Science 373 (6561), 1336.

Chen, W., Bai, R., Zhao, B., Zhou, X., Zhao, F., Xiao, Y., 2026. Redox-active antioxidants enable highly stable bio-electrochemical systems. Bioresour. Technol. 447.

Chen, Y.-C., Li, Y.-T., Lee, C.-L., Kuo, Y.-T., Ho, C.-L., Lin, W.-C., Hsu, M.-C., Long, X., Chen, J.-S., Li, W.-P., Su, C.-H., Okamoto, A., Yeh, C.-S., 2023. Electroactive membrane fusion-liposome for increased electron transfer to enhance radiodynamic therapy. Nat. Nanotechnol. 18 (12), 1492–1501.

Cordova, C.D., Schicklberger, M.F.R., Yu, Y., Spormann, A.M., 2011. Partial functional replacement of CymA by SirCD in *Shewanella oneidensis* MR-1. J. Bacteriol. 193 (9), 2312–2321.

Ezraty, B., Gennaris, A., Barras, F., Collet, J.-F., 2017. Oxidative stress, protein damage and repair in bacteria. Nat. Rev. Microbiol. 15 (7), 385–396.

Feng, X., Sun, W., Kong, L., Gao, H., 2019. Distinct roles of *Shewanella oneidensis* thioredoxin in regulation of cellular responses to hydrogen and organic peroxides. Appl. Environ. Microbiol. 85 (21), e01700–e01719.

Fredrickson, J.K., Romine, M.F., Beliaev, A.S., Auchtung, J.M., Driscoll, M.E., Gardner, T. S., Nealson, K.H., Osterman, A.L., Pinchuk, G., Reed, J.L., Rodionov, D.A., Rodrigues, J.L.M., Saffarini, D.A., Serres, M.H., Spormann, A.M., Zhulin, I.B., Tiedje, J.M., 2008. Towards environmental systems biology of *Shewanella*. Nat. Rev. Microbiol. 6 (8), 592–603.

Gang, H., Xiao, C., Xiao, Y., Yan, W., Bai, R., Ding, R., Yang, Z., Zhao, F., 2019. Proteomic analysis of the reduction and resistance mechanisms of *Shewanella oneidensis* MR-1 under long-term hexavalent chromium stress. Environ. Int. 127, 94–102.

Gao, H., Yang, Z.K., Barua, S., Reed, S.B., Romine, M.F., Nealson, K.H., Fredrickson, J.K., Tiedje, J.M., Zhou, J., 2009. Reduction of nitrate in *Shewanella oneidensis* depends on atypical NAP and NRF systems with NapB as a preferred electron transport protein from CymA to NapA. ISME J. 3 (8), 966–976.

Gralnick, J.A., Vali, H., Lies, D.P., Newman, D.K., 2006. Extracellular respiration of dimethyl sulfoxide by *Shewanella oneidensis* strain MR-1. PNAS 103 (12), 4669–4674.

Harnisch, F., Deutzmann, J.S., Boto, S.T., Rosenbaum, M.A., 2024. Microbial electrosynthesis: opportunities for microbial pure cultures. Trends Biotechnol. 42 (8), 1035–1047.

Holm, A.K., Blank, L.M., Oldiges, M., Schmid, A., Solem, C., Jensen, P.R., Vemuri, G.N., 2010. Metabolic and transcriptional response to cofactor perturbations in *Escherichia coli*. J. Biol. Chem. 285 (23), 17498–17506.

Hou, L., Zheng, B., Jiang, Z., Hu, Y., Shi, L., Dong, Y., Jiang, Y., 2024. The dmsEFABGH operon encodes an essential and modular electron transfer pathway for extracellular iodate reduction by *Shewanella oneidensis* MR-1. Microbiol. Spectrum 12 (8).

Imlay, J.A., 2013. The molecular mechanisms and physiological consequences of oxidative stress: lessons from a model bacterium. Nat. Rev. Microbiol. 11 (7), 443–454.

Kouzuma, A., Hashimoto, K., Watanabe, K., 2012. Influences of aerobic respiration on current generation by *Shewanella oneidensis* MR-1 in single-chamber microbial fuel cells. Biosci. Biotech. Bioch. 76 (2), 270–275.

Light, S.H., Su, L., Rivera-Lugo, R., Cornejo, J.A., Louie, A., Iavarone, A.T., Ajo-Franklin, C.M., Portnoy, D.A., 2018. A flavin-based extracellular electron transfer mechanism in diverse Gram-positive bacteria. Nature 562 (7725), 140.

Lin, X., Yang, F., You, L.-X., Wang, H., Zhao, F., 2021. Liposoluble quinone promotes the reduction of hydrophobic mineral and extracellular electron transfer of *Shewanella oneidensis* MR-1. Innovation (Cambridge (Mass.)) 2 (2), 100104.

Liu, Q., Ding, Q., Xu, W., Zhang, Y., Zhang, B., Yu, H., Li, C., Zhang, J., You, Z., Tang, R., Wu, D., Zhao, C., Cao, Y., Lu, W., Li, F., Song, H., 2023. Engineering cell-electrode interfacial electron transfer to boost power generation of electroactive biofilm. Nano Energy 117, 108931.

Lloyd, D., 1993. Aerobic denitrification in soils and sediments - from fallacies to facts. Trends Ecol. Evol. 8 (10), 352–356.

Logan, B.E., 2009. Exoelectrogenic bacteria that power microbial fuel cells. Nat. Rev. Microbiol. 7 (5), 375–381.

Lovley, D.R., 2006. Bug juice: harvesting electricity with microorganisms. Nat. Rev. Microbiol. 4 (10), 797.

Lu, M., Chan, S., Babanova, S., Bretschger, O., 2017. Effect of oxygen on the per-cell extracellular electron transfer rate of *Shewanella oneidensis* MR-1 explored in bioelectrochemical systems. Biotechnol. Bioeng. 114 (1), 96–105.

Lu, Z., Imlay, J.A., 2021. When anaerobes encounter oxygen: mechanisms of oxygen toxicity, tolerance and defence. Nat. Rev. Microbiol. 19 (12), 774–785.

Marsili, E., Baron, D.B., Shikhare, I.D., Coursolle, D., Gralnick, J.A., Bond, D.R., 2008. *Shewanella* secretes flavins that mediate extracellular electron transfer. PNAS 105 (10), 3968–3973.

McKenzie, R.M., 1971. Synthesis of birnessite, cryptomelane, and some other oxides and hydroxides of manganese. Mineral. Mag. 38 (296), 493.

Mevers, E., Su, L., Pishchany, G., Baruch, M., Cornejo, J., Hobert, E., Dimise, E., Ajo-Franklin, C.M., Clardy, J., 2019. An elusive electron shuttle from a facultative anaerobe. eLife 8, e48054.

Myers, C.R., Nealson, K.H., 1988. Bacterial manganese reduction and growth with manganese oxide as the sole electron-acceptor. Science 240 (4857), 1319–1321.

Norman, M.P., Edwards, M.J., White, G.F., Burton, J.A.J., Butt, J.N., Richardson, D.J., Louro, R.O., Paquete, C.M., Clarke, T.A., 2023. A cysteine pair controls flavin reduction by extracellular cytochromes during anoxic/oxic environmental transitions. MBio 14 (1), e02589–e02622.

Ringeisen, B.R., Ray, R., Little, B., 2007. A miniature microbial fuel cell operating with an aerobic anode chamber. J. Power Sources 165 (2), 591–597.

Shi, L., Dong, H., Reguera, G., Beyenal, H., Lu, A., Liu, J., Yu, H.-Q., Fredrickson, J.K., 2016. Extracellular electron transfer mechanisms between microorganisms and minerals. Nat. Rev. Microbiol. 14 (10), 651–662.

Su, L., Fukushima, T., Ajo-Franklin, C.M., 2020. A hybrid cyt *c* maturation system enhances the bioelectrical performance of engineered *Escherichia coli* by improving the rate-limiting step. Biosens. Bioelectron. 165, 112312.

Tejedor-Sanz, S., Stevens, E.T., Li, S., Finnegan, P., Nelson, J., Knoesen, A., Light, S.H., Ajo-Franklin, C.M., Marco, M.L., 2022. Extracellular electron transfer increases fermentation in lactic acid bacteria via a hybrid metabolism. eLife 11, e70684.

TerAvest, M.A., Rosenbaum, M.A., Kotloski, N.J., Gralnick, J.A., Angenent, L.T., 2014. Oxygen allows *Shewanella oneidensis* MR-1 to overcome mediator washout in a continuously fed bioelectrochemical system. Biotechnol. Bioeng. 111 (4), 692–699.

Trouwborst, R.E., Clement, B.G., Tebo, B.M., Glazer, B.T., Luther, G.W., Iii., 2006. Soluble Mn(III) in suboxic zones. Science 313 (5795), 1955–1957.

Xiao, Y., Chen, G., Chen, Z., Bai, R., Zhao, B., Tian, X., Wu, Y., Zhou, X., Zhao, F., 2021. Interspecific competition by non-exoelectrogenic *Citrobacter freundii* An1 boosts bioelectricity generation of exoelectrogenic *Shewanella oneidensis* MR-1. Biosens. Bioelectron. 194, 113614.

Xiao, Y., Zhang, E., Zhang, J., Dai, Y., Yang, Z., Christensen, H.E.M., Ulstrup, J., Zhao, F., 2017. Extracellular polymeric substances are transient media for microbial extracellular electron transfer. Sci. Adv. 3 (7), e1700623.

Yang, C., Aslan, H., Zhang, P., Zhu, S., Xiao, Y., Chen, L., Khan, N., Boesen, T., Wang, Y., Liu, Y., Wang, L., Sun, Y., Feng, Y., Besenbacher, F., Zhao, F., Yu, M., 2020. Carbon dots-fed *Shewanella oneidensis* MR-1 for bioelectricity enhancement. Nat. Commun. 11 (1), 1379.

Zhu, T., Cheng, Z., Yu, S., Li, W., Liu, D., Yu, H., 2022. Unexpected role of electron-transfer hub in direct degradation of pollutants by exoelectrogenic bacteria. Environ. Microbiol. 24 (4), 1838–1848.